Thermochimica Acta, 31 (1979) 323–339

CALORIMETRIC DETERMINATION OF EQUILIBRIUM PHASE DIAGRAMS OF INORGANIC SYSTEMS

M. GAUNE-ESCARD*

Laboratoire de Dynamique et Thermophysique des Fluides, L.A. 72, Université de Provence, Centre de St Jérôme, Rue Henri Poincaré, 13397 Marseille, Cédex 4 (France)

J. P. BROS

Laboratoire de Thermodynamique des Systèmes Métalliques à composants multiples, Université de Provence, 3, Place Victor-Hugo, 13331 Marseille, Cédex 3 (France)

(Received 27 July 1978)

ABSTRACT

Calorimetric isobaric determination of the heat involved during mixing processes gives the concentration dependence of the enthalpy of mixing $\Delta H_M = f(x)$ and also, under particular conditions, some liquidus concentrations of the phase diagram.

For some simple typical diagrams (with a eutectic point or miscibility gaps, or a definite compound etc.) direct calorimetric experiments at many temperatures give the liquidus (e.g. NaBr–$NaNO_3$, KBr–KNO_3, NaB–KNO_3, KBr–$NaNO_3$, Ga–Hg, Ga–Sb).

For more complicated or multicomponent systems, the setting up of the equilibrium phase diagram needs both experimental measurements and thermodynamic calculations (e.g. Ga–In–Sb).

INTRODUCTION

General physical or chemical methods allow the determination of the equilibrium lines of a phase diagram. At present, thermal analysis is the most common method used.

It must be recalled that the isobaric determination of an equilibrium phase diagram for an organic or inorganic 2, 3 or n component system is based on the variations of a physical or n chemical parameter plotted against either temperature or concentration. Figure 1(a) shows a very simple type of condensed binary system; by following the thermal effects arising from a linear change of temperature against time (isopleth XX'), a thermal analysis thermogram of a well-known shape[1] is obtained [Fig. 1(b)]. Points a' and b' correspond to the intersections of the equilibrium

* To whom correspondence should be addressed.

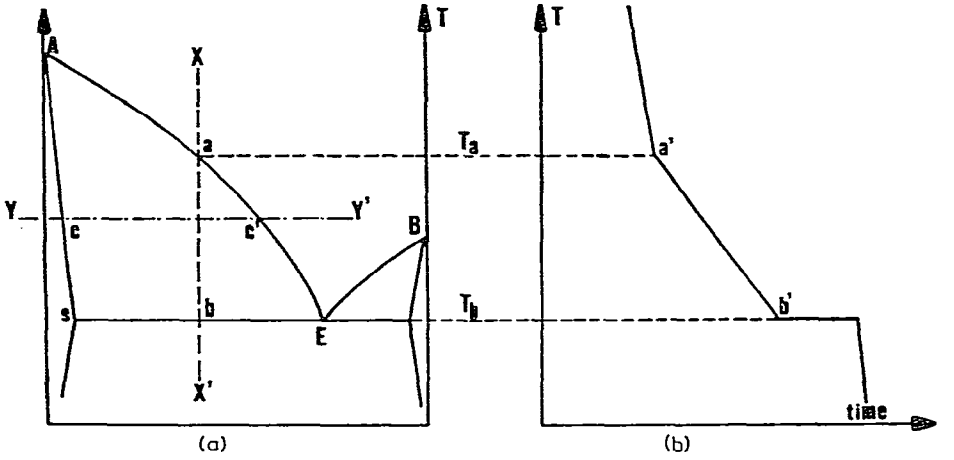

Fig. 1. (a) Schema of an equilibrium phase diagram exhibiting eutectic point. (b) Curve of differential thermal analysis $T = f(t)$: temperature against time.

lines AE and ES of the phase diagram. In the same way, the quilibrium points c and c' can be detected by following the change in a physical parameter such as electrical conductivity, viscosity, etc.

The choice of a suitable method for the determination of equilibrium lines depends on many factors such as physical and chemical properties of components (reactivity, volatility, etc.), shape of equilibrium phase diagrams, etc. The determination, for instance, of a liquid miscibility gap or of a liquidus line with a large slope is critical by thermal analysis and other methods seem more appropriate.

In many cases, calorimetry and more particularly microcalorimetry is able to give information allowing us either to obtain directly the coordinates of the equilibrium points or to calculate indirectly some equilibrium lines of a phase diagram, this will be shown in the following sections.

PRINCIPLE OF THE METHOD

For the sake of clarity this study has been limited to binary and ternary mixtures but the generalization to n-component systems can be done without much difficulty.

At constant temperature and pressure, the measurement of the enthalpy of formation ΔH_M of a liquid single phase binary mixture against the mole fraction X_A of one component is relatively easy[2-7]; the plot of $\Delta H_M = f(X_A)$ function has a quasi-parabolic shape. This same function, when single and many phase regions appear successively, exhibits then a characteristic shape which can easily be explained by the "lever rule".

Figure 2 gives an idea of the shape of the $\Delta H_M = f(X_A)$ curve obtained at several temperatures and for different liquidus kinds. Only three kinds of fairly simple equilibrium diagram have been kept back for this theoretical example [Fig. 2(a)–(c)]. The broken lines on the figures correspond to the experimental temperatures T_1 and T_2 for which, over the whole concentration range, the mixtures

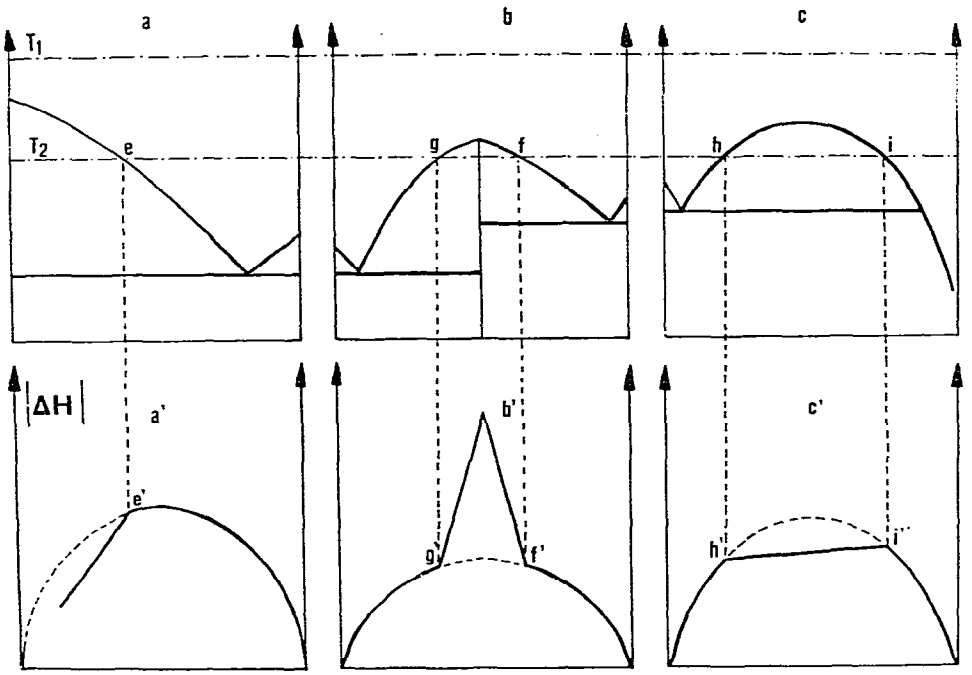

Fig. 2. (a)–(c) Schema of three liquidus of phase diagram (with eutectic point, definite compound and miscibility gap, respectively). (a')–(c') Shape of the enthalpy of mixing functions (ΔH_M) plotted against concentration X at experimental temperatures T_1 (dashed line curve) and T_2 (full line curve).

are either single phase (T_1) or two phase (T_2). The diagrams 2(a')–(c') illutrate the shape of $\Delta H = f(X_A)$ curves obtained at T_1 and at T_2. We used the simplifying hypothesis, which is usually accepted, that the enthalpy of mixing does not change with temperature. Each liquidus crossing corresponds to an angular point (g–g', h–h', etc.) on the $\Delta H = f(X_A)$ curve. The break points h' and i' refer to the intersection of $\Delta H_M = f(X_A)$ — quasi-parabolic curve for a liquid single phase region — with the straight line $h'i'$. The segment $h'i'$ arises from the linear variation (lever rule) of the amounts of the conjugated liquids L_1 and L_2, the enthalpies of formation of which are $\Delta H_M^{L_1}$ and $\Delta H_M^{L_2}$. For the second diagram, the linear parts correspond to the existence of the definite compound A_xB_y. This microcalorimetric determination can therefore provide not only the coordinates of equilibrium points but also the thermodynamic quantities of formation of these mixtures, quantities which will be useful in the calculation of equilibrium phase diagrams. This technique is generally completed by thermal differential analysis performed with the same apparatus and the same sample.

APPARATUS AND TECHNIQUES

Apparatus

The principle of the microcalorimeter was proposed in 1922 by Tian[8] but only some twenty years later, thanks to Calvet[9], did this apparatus become easy to use over a very large temperature range (100–1300 K). This isoperibolic calorimeter has

been described often, so only the characteristics vital to this paper are recalled here.

A microcalorimeter is mainly composed of the following parts.

(1) An external steel enclosure surrounding a cylindrical furnace; four resistors, one on the bottom, one on the top, two on the cylindrical/walls, provide the heating.

(2) A calorimeter block, made of either aluminium or copper for medium temperature apparatus (M.T.), either Kanthal or alumina for high temperature apparatus (H.T.). This block contains two or four cavities for the thermopiles and is surrounded by many enclosures acting as thermal and electrical shields.

(3) Each thermopile consists of a cylindrical tube closed at the bottom, the so-called "calorimeter cell" of silver (M.T.) or alumina (H.T.), on which the "hot" thermocouple junctions lay, the "cold" junctions being in contact with the calorimetric block. The kind of thermocouple depends on the temperature of the microcalorimeter in use (Pt/Pt–10% Rh for H.T.).

The size of the cells (generally 17 mm in diameter and 80 mm high) and the shape of the thermocouple supports are dictated by technical considerations but one condition has to be respected: the maximum thermal flux must be integrated adequately by the thermocouples.

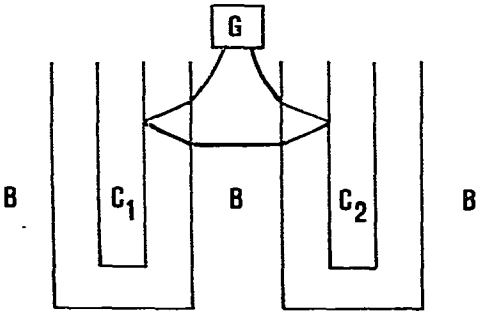

Fig. 3. Schematic diagram of differential joining-up of Calvet calorimeter. C_1, C_2, calorimeter cell; B, calorimeter block.

In order to obtain a good stability of the apparatus with regard to time and temperature, the two thermopiles are connected in opposition (Fig. 3); any exterior thermal perturbation is thus eliminated. The strip-chart recorder is of a galvanometric kind (Sefram). The furnace is maintained at constant temperature with an electronic regulator; the sensing element is either a thermistor or a thermocouple, located as close as possible to the heating element. The experimental temperature is controlled by means of a thermocouple situated in the calorimetric block center.

A linear temperature programmer is added to the regulator; the apparatus may be used then as a differential enthalpic analyzer but its thermal insensitivity is such that the heating speed never exceeds a few degrees an hour; this inconvenience is largely compensated for by its great sensitivity and its large experimental volume. The cell used for differential enthalpic analysis is shown in Fig. 4.

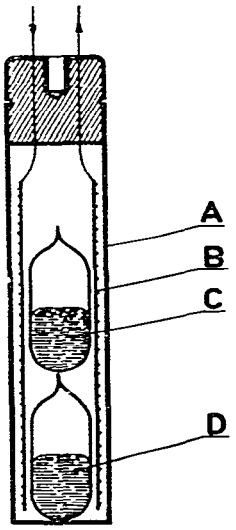

Fig. 4. Section of a microcalorimetric cell used for differential enthalpimetric analysis of the phase transitions. A, cell; B, calibration resistance; C and D, sample).

Experimental techniques

The experimental techniques worked out in calorimetry for the determination of enthalpies of mixing are numerous. For all of them, it is essential to eliminate all effects arising generally from material–atmosphere interactions (oxidizing, hygroscopic, etc. substances), from solvent or solute–crucible interactions, from difficulties of mixing (A and B with very different densities), from the stirring necessary to homogenise the final product, from the introduction of a solute at a temperature different from that of the solvent, etc. In order to solve these specific problems, some researchers created not only various devices but sometimes built special calorimeters[10–12].

We indicate the main techniques for systems the components of which melt above ambient temperature.

The former and also the easier method to work out, the so-called "drop method", has been described at length by Kubachewski[2]; it consists of dropping into the liquid substance A, considered as a solvent and maintained at the experimental temperature T_E, a known amount of substance B, previously stabilized at temperature T_0 (generally ambient temperature). This technique is very simple and has been applied to a microcalorimeter [Fig. 5(a)]; the recorded thermal effect (Q_p) is the sum of three effects arising from heat of mixing (Q_M), heat of fusion (Q_F) and that necessary to raise the temperature of sample B (mass m) from

$$T_0 \text{ to } T_E, \left(m \int_{T_0}^{T_E} C_p \, dT \right), \text{ i.e.}$$

$$Q_p = Q_M + Q_F + m \int_{T_0}^{T_E} C_p \, dT$$

Unfortunately, for some systems, uncertainty in the terms Q_F and $m \int_{T_0}^{T_E}$ is of the same order of magnitude as Q_M, which removes any meaning in the Q_M measurement.

In order to palliate these inconveniences, we developed an *indirect drop method* [Fig. 5(b)]. The sample B falls into the funnel, F; its fall is guided by tube T, the lower end of which obstructs the funnel. When B is in thermal equilibrium with the whole, a simple vertical movement of T allows mixing to take place. We have been able to include a stirring device for the mixture[7]. In order to keep the samples either under vacuum, or under an inert atmosphere (argon grade U*) the upper part of the system involves a set of taps and joints, and all movement of the drop tube and the stirrer is electromagnetically controlled.

The *break-off ampoule* method as well as the *suspended crucible* method [see Figs. 5(c) and (d)] have often been used with molten salt mixtures. The pyrex or quartz ampoule has to be thin enough to break with a single press. The thermal effect arising from the ampoule break-off [Fig. 5(c)] or from the small crucible drop [Fig. 5(d)] is very small but reproducible.

Enthalpies of mixing may also be determined using the method of *continuous*

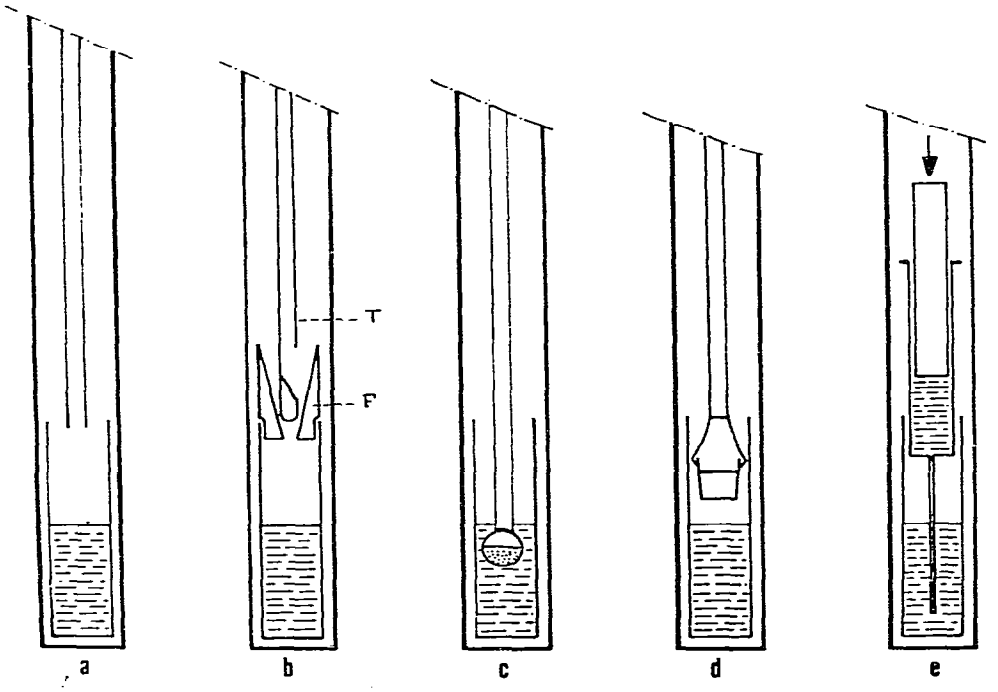

Fig. 5. Some diagrams of devices usually used for microcalorimetry. a, direct drop method; b, indirect drop method, the tip of the tube T stops the sample drop in the funnel F; c, break-off ampoule method; d, suspended crucible method; e, injection of two liquids into the cell.

* Air Liquide Company.

injection of a liquid A into the solute B [Fig. 5(e)] Started by Leydet[13], this technique has been used mainly for aqueous solutions; a few experiments will give enthalpy values over the whole concentration range. The application of this method at high temperature is possible but the choice of materials for the construction of the cell remains critical. Kleppa[14] used a somewhat similar device for ionic mixtures but without continuous output.

A systematic study of calibration coefficients by the Joule effect or by dropping a metal of known heat capacity[15]. and the reproducibility of results has pointed out that in the temperature range 200–750 °C, the precision of results is between 2 and 6%. At higher temperatures, between 800 and 1500 °C, precision, which greatly depends on the system studied may reach 10%.

RESULTS

To illustrate the use of this method, we choose to study some mixtures having typical equilibrium phase diagrams, viz.

(1) MBr–MNO_3 systems (M = Na or K) with an eutectic point;

(2) Ga–Hg system with a liquid miscibility gap; and

(3) Ga–Sb system with a definite compound.

Moreover, we will show that the thermodynamic quantities so obtained enable us to calculate the liquidus of more complex systems, e.g. the Ga–In–Sb ternary system.

MBr–MNO_3 systems (M = Na or K)

These four systems (NaBr–$NaNO_3$, KBr–KNO_3, NaBr–KNO_3, KBr–$NaNO_3$) are, respectively, two limiting common ion binary systems and the two diagonals of the molten-salt reciprocal mixture Na^+, $K^+//NO_3^-$, Br^-.

For all these systems, the equilibrium phase diagram exhibits an eutectic point[16].

The enthalpies of formation, ΔH, of liquid mixtures have been carried out with the break-off ampoule method. The experimental results given in Table 1 correspond to the formation of a liquid mixture from solid bromide and liquid nitrate

$$x\,MBr(s) + (1 - x)\,MNO_3(l) = (x\,MBr\,(1 - x)\,MNO_3)(l)$$

with M = Na or K.

The choice of this solid–liquid reference was necessary because of the large difference between the melting points of alkali bromides and nitrates.

Before their use in the calorimeter, all the salts ("suprapur" reagents from Merck) were dried at 425 K.

In Figs. 6 and 7, for each system, the variation of the enthalpy of formation, ΔH, has been plotted against the mole fraction of alkali bromide; each curve exhibits two distinct regions, the left part corresponding to the liquid single phase domain of

TABLE 1

EXPERIMENTAL ENTHALPIES OF MIXING (ΔH) AGAINST MOLE FRACTION OF MBr (x_{Br^-}) IN MBr–MNO_3 MOLTEN SALT SYSTEMS (WITH M = Na, K)

x_{Br^-}	ΔH (*kcal mole*$^{-1}$)	x_{Br^-}	ΔH (*kcal mole*$^{-1}$)	x_{Br^-}	ΔH (*kcal mole*$^{-1}$)
NaBr–NaNO$_3$		*KBr–KNO*$_3$		*NaBr–KNO*$_3$	
0.0093	0.055	0.0083	0.04	0.0101	0.04
0.0100	0.060	0.0090	0.05	0.0103	0.05
0.0105	0.065	0.0091	0.05	0.0105	0.05
0.0114	0.070	0.0304	0.15	0.0106	0.05
0.0634	0.380	0.0567	0.32	0.0125	0.06
0.0732	0.440	0.0729	0.40	0.0788	0.37
0.0761	0.470	0.0869	0.51	0.1194	0.58
0.0799	0.500	0.1018	0.56	0.1539	0.77
0.0895	0.560	0.1238	0.67	0.1610	0.78
0.1001	0.650	0.1573	0.77	0.1802	0.85
0.1201	0.770	0.1947	0.70	0.2315	1.15
0.1205	0.710	0.3107	0.59	0.2507	1.20
0.1210	0.735	0.3758	0.52	0.2607	1.29
0.1353	0.840			0.2738	1.34
0.1606	0.996	*KBr–NaNO*$_3$		0.3016	1.45
0.1728	1.050	0.0054	0.03	0.3050	1.50
0.2018	1.210	0.0077	0.05	0.3147	1.52
0.2488	1.414	0.0166	0.10	0.3375	1.57
0.2499	1.420	0.0871	0.51	0.3611	1.70
0.2627	1.330	0.1034	0.60	0.3778	1.79
0.2799	1.320	0.1071	0.65	0.3989	2.01
0.3059	1.550	0.1144	0.68	0.4117	2.03
0.3223	1.470	0.1685	0.98	0.4358	2.10
0.3385	1.410	0.1777	1.05	0.4379	2.09
0.3398	1.370	0.1833	1.08	0.4380	2.12
0.3458	1.460	0.1876	1.10	0.4497	2.09
0.3576	1.456	0.2136	1.25	0.4660	2.24
0.3831	1.310	0.2176	1.31	0.4719	2.17
0.3850	1.430	0.2378	1.44	0.4815	2.23
0.4277	1.270	0.2890	1.68	0.4823	2.28
0.4319	1.280	0.2913	1.73	0.5159	2.19
0.4557	1.220	0.2933	1.69	0.5204	2.13
0.4962	1.180	0.2954	1.67	0.5221	2.10
0.5037	1.150	0.3042	1.78	0.5377	2.16
0.5051	1.160	0.3387	1.97	0.5767	2.13
0.5160	1.100	0.3649	2.10	0.5953	2.01
0.5227	1.100	0.3709	2.17	0.6168	1.91
0.5354	1.050	0.4145	2.35	0.6512	1.72
0.6770	0.786	0.5084	2.41	0.6563	1.73
0.6893	0.720	0.5177	2.42	0.7104	1.53
0.7494	0.607	0.5119	2.28	0.7316	1.40
0.7513	0.600	0.6563	1.72		
		0.6880	1.52		

the phase diagram and the other one to the liquid–solid domain, so the angular point corresponds to the equilibrium concentration at the experimental temperature.

The lower part of the same Figs. 6 and 7 are the experimental phase diagrams of the MBr–MNO_3 systems as taken from Nyankowskaya[16]; it can be seen that the agreement between the experimental concentration and that obtained from our calorimetric measurements is satisfactory. For the NaBr–KNO_3, which is the unstable pair[16] of the Na^+, $K^+//NO_3^-$,Br^- reciprocal molten salt mixture, the enthalpy of mixing plot on Fig. 7(a) exhibits a scattering of experimental points; this scattering probably arises from a very slow equilibrium setting of the system since the Gibbs energy ΔG associated with the reaction

$$NaBr + KNO_3 = NaNO_3 + KBr$$

is very small at the experimental temperature (723 K).

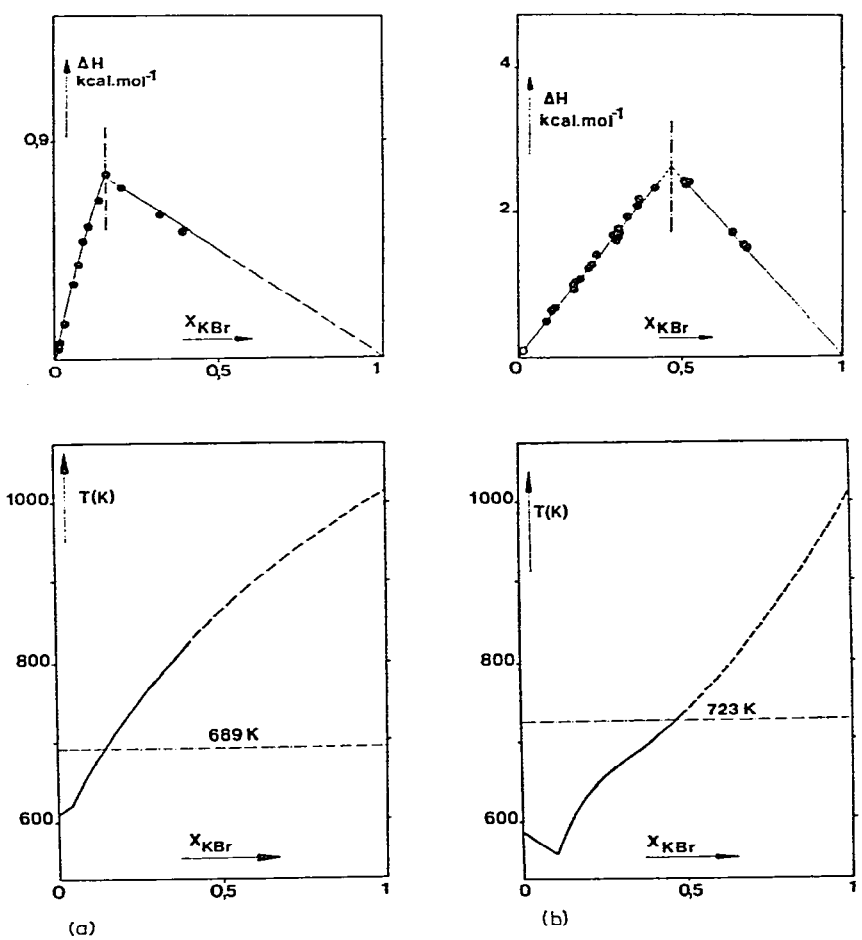

Fig. 6. (a), KNO_3–KBr system $\Delta H = f(X)$ and liquidus of the phase diagram; (b), $NaNO_3$–KBr system $\Delta H = f(X)$ and liquidus of the phase diagram.

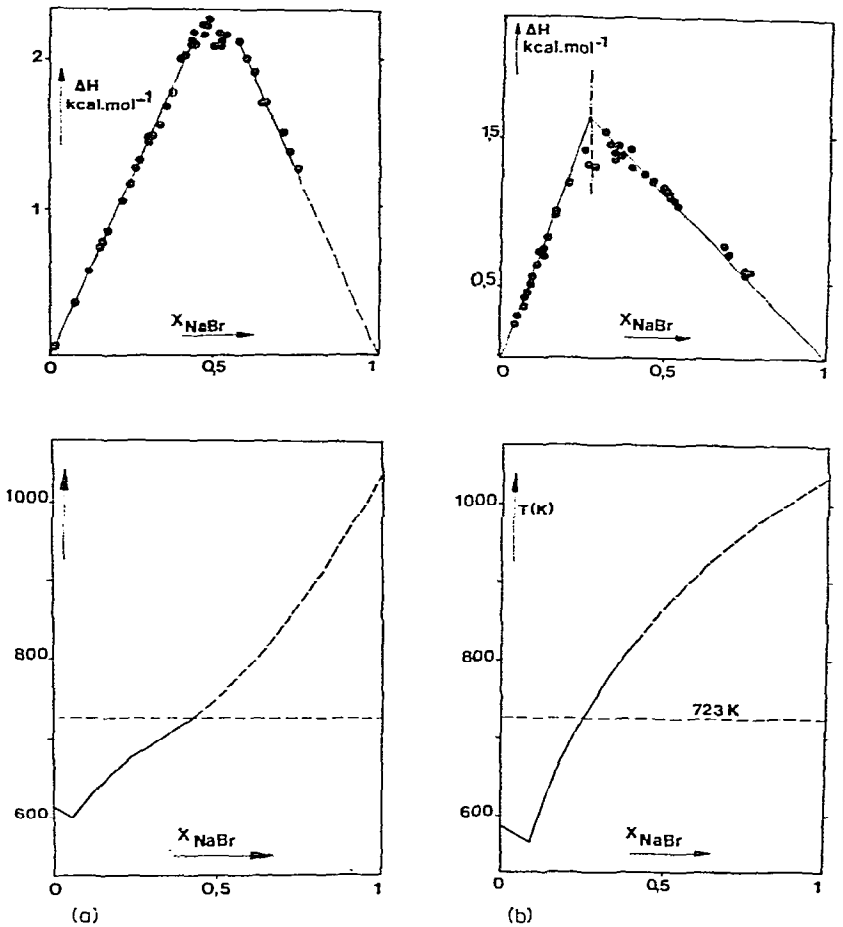

Fig. 7. (a), KNO_3–NaBr system $\Delta H = f(X)$ and liquidus of the phase diagram; (b), $NaNO_3$–NaBr system $\Delta H = f(X)$ and liquidus of the phase diagram.

Gallium–mercury system

For this system, an important miscibility gap exists in the liquid state; its critical temperature seems to be situated at about 473 K[17, 18] (Fig. 8).

The experimental technique chosen is the break-off ampoule one. Because of the volatility of mercury, an atmosphere of inert gas (argon grade U) is maintained in

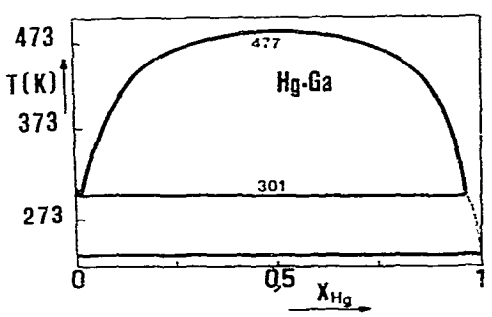

Fig. 8. Equilibrium phase diagram of Ga–Hg system.

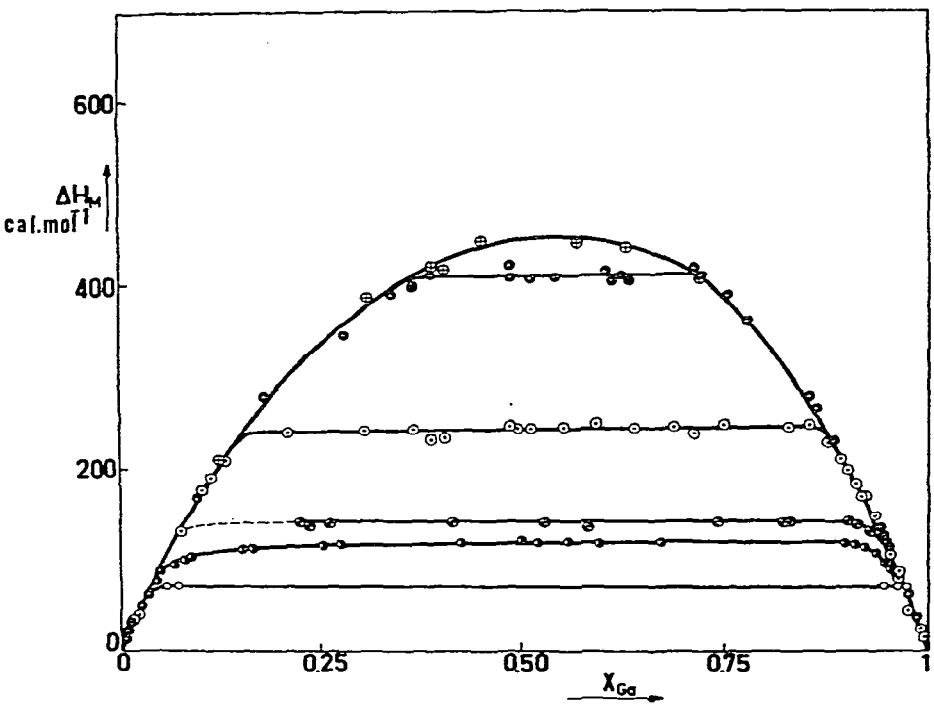

Fig. 9. Enthalpies of formation of Ga–Hg mixtures at many temperatures (○, 313 K; ◑, 353 K; ◕, 373 K; ⊙, 423 K; ○, 467 K; ⊕, 478 K).

TABLE 2

EXPERIMENTAL ENTHALPIES OF MIXING (ΔH), IN CAL MOLE^{-1}, AGAINST MOLE FRACTION OF Ga (x_{Ga}) AT SEVERAL TEMPERATURES IN THE Ga–Hg SYSTEM

T(K)	x_{Ga} *0*	*0.1*	*0.2*	*0.3*	*0.4*	*0.5*	*0.6*	*0.7*	*0.8*	*0.9*	*1*
313	0	75	75	75	75	75	75	75	75	75	0
353	0	110	112	117	117	117	117	117	117	114	0
372	0	142	142	142	142	142	142	142	142	138	0
423	0	180	244	244	244	244	244	244	244	200	0
466	0	180	300	370	420	420	420	420	340	200	0
478	0	180	300	370	420	440	440	420	340	200	0

TABLE 3

Ga–Hg SYSTEM. EXPERIMENTAL LIQUIDUS COORDINATES AND COMPARISON WITH PREVIOUS STUDIES

	T(K) *313*	*353*	*373*	*423*	*466*	*Ref.*
x_{Ga}	0.045	0.065	0.085	0.135	0.285	18
x_{Ga}	0.975	0.955	0.945	0.880	0.670	
x_{Ga}	0.041	0.066	0.082	0.150	0.300	17
x_{Ga}	0.980	0.950	0.935	0.860	0.672	
x_{Ga}	0.042	0.063	0.935	0.150	0.360	This work
x_{Ga}	0.976	0.954	0.938	0.870	0.720	

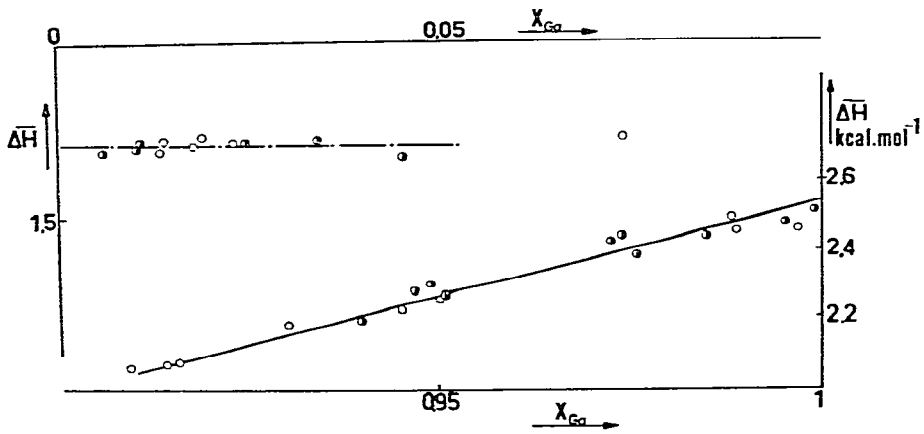

Fig. 10. Partial enthalpies of dissolution of gallium in mercury and of mercury in gallium ○, 423 K; ◑, 493 K.

the cell. Moreover, both metals are covered with a previously degasified oil layer; the metals and alloys do not show any oxidation traces after the experiment.

The calorimeter was calibrated by the Joule effect; all the experiments have been performed at 313, 353, 373, 423, 467 and 478 K. As shown in Fig. 9, the large number of experiments performed reveals the miscibility gap ($L_1 + L_2$). All the calorimetric results are plotted on these curves and Table 2 shows the enthalpies of mixing found for increments of 0.1 mole fraction of gallium. The quasi-horizontal level which corresponds to the liquid two-phase domain disappeared completely at 478 K.

Table 3 enables us to compare the critical temperatures found either by Amarel[18] or by Predel[17]; we included those obtained by calorimetry: the agreement is satisfactory. The maximum value of the enthalpy of mixing is 440 cal mole^{-1} whereas Predel obtained 380 cal mole^{-1}.

By extrapolation of measurements performed at low concentrations (see Fig. 10), we determined the limiting partial enthalpies of gallium in mercury and of mercury in gallium. At 466 K, we find that $(\Delta\bar{H}_{Ga})^{\infty}_{Hg} = 1720$ cal mole^{-1} and $(\Delta\bar{H}_{Hg})^{\infty}_{Ga} = 2550$ cal mole^{-1}. At 313 K, the values are, respectively, 1900 cal mole^{-1} and 2600 cal mole^{-1}.

From equilibrium temperatures given by Amarell[18], we calculated the excess limiting partial enthalpy of gallium in mercury: we found it to be 1780 cal mole^{-1}, which is reasonably close to the experimental value.

These results have also to be compared with Marco's[19]; at 293 K, the limiting partial enthalpy of gallium in mercury is 3200 cal mole^{-1}.

Gallium–antimony system

The equilibrium phase diagram has been determined by several researchers[20–24]: it exhibits two eutectic points and a definite compound GaSb which melts at 985 K (see Fig. 11).

In the homogeneous liquid phase, some direct calorimetric measurements have been performed at 1003 K[24] and 1023 K[25]. We repeated these measurements at 995 K

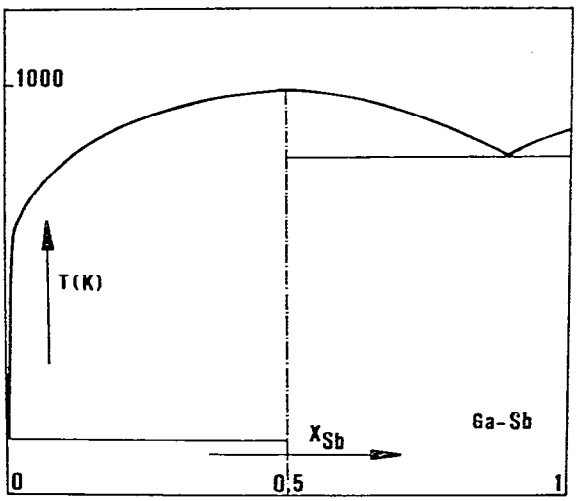

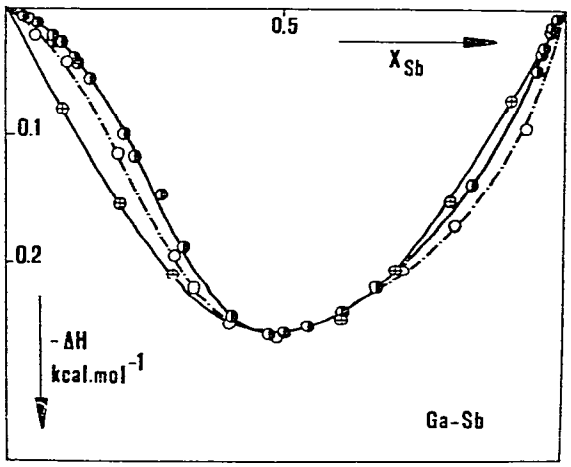

Fig. 11. Equilibrium phase diagram of Ga–Sb system.

Fig. 12. Ga–Sb system: $\Delta H_M = f(X_{Sb})$. ◑: 995 K; ⊕: 1003 K (from Yasawa[24]); ○: 1023 K (from Predel[25]).

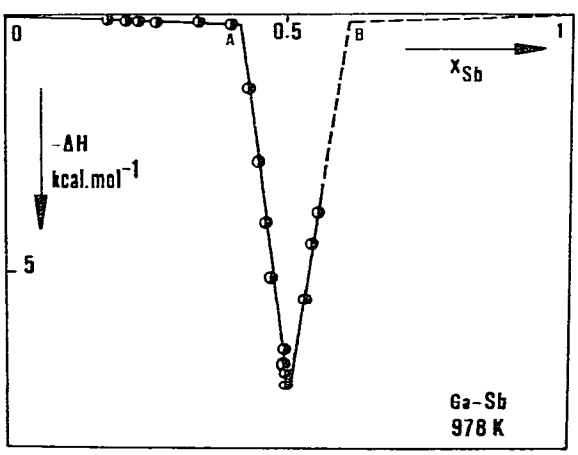

Fig. 13. Ga–Sb system, $\Delta H_M = f(X_{Sb})$ at 978 K.

using an indirect drop method[26]. Figure 12 shows all these results. Although for mole fraction $x_{Sb} = 0.5$ there is excellent agreement between our value and those already published, the general appearance of the curve is clearly different. The analytical expression of the enthalpy of formation in the liquid homogeneous region is given in the next paragraph.

At 978 K, using only the indirect drop method, we have determined the enthalpy of formation of this system over the whole concentration range. From $x_{Sb} = 0$ to $x_{Sb} = 0.415$, we observed the same curve as previously, corresponding to the formation of a liquid single-phase mixture; for $x_{Sb} > 0.415$ the appearance of the GaSb solid phase corresponds to the linear part on the curve $\Delta H = f(x_{Sb})$ (Fig. 13).

So, from this plot we obtained the enthalpy of formation of the GaSb compound at 978 K

$\Delta H_f(978\ K) = -(7000 \pm 300)$ cal mole^{-1}

and also, from points A and B, the equilibrium concentrations at the same temperature.

Gallium–indium–antimony system

The value of thermodynamic functions of mixing may also enable, in some cases, the estimation of the liquidus. The Ga–In–Sb system has been chosen as an example. For this system, the only experimental thermodynamic quantities obtained by differential thermal analysis, refer on, the one hand, to Ga–In–Sb solution at 910 K and on the other hand, to the Ga–Sb and In–Sb quasi-binary solutions.

The liquidus temperature was measured at some compositions by Blom[27], Antypas[28], Joullie[29] and Koster[20]. The GaSb–InSb equilibrium phase diagram was studied by Blom[27], Woolley[30–32], Nikitina[33] and Trumbore[34].

The experimental results obtained for the Ga–In, Ga–Sb and Ga–In–Sb systems are recalled below as equations. For the In–Sb system, we used the thermodynamic quantities compiled by Hultgren[35] and which are consistent.

Ga–In system. A critical study of results available from several authors[36–38] leads to the following relationship.

$\Delta H_M = 1060\, x_{In}\, x_{Ga}$ cal mole^{-1}
$\Delta S_M^{XS} = 0.25\, x_{In}\, x_{Ga}$ cal mole^{-1}K^{-1}

Ga–Sb system. We kept the two equations.

$\Delta H_M = x_{Ga}\, x_{Sb}\,(-3773.45\, x_{Sb}^3 + 7690.44\, x_{Sb}^2 + 5162.35\, x_{Sb} + 127.01)$ cal mole^{-1}
$\Delta S_M^{XS} = x_{Ga}\, x_{Sb}\,(-3.773\, x_{Sb}^3 + 5.862\, x_{Sb}^2 - 3.455\, x_{Sb} + 1.159)$ cal mole^{-1} K^{-1}

In–Sb system. Hultgren[35] proposed for the excess enthalpy and entropy of mixing the relationships

$\Delta H_M = x_{In}\, x_{Sb}\,(-5950.45\, x_{Sb}^3 + 11152.29\, x_{Sb}^2 - 4726.20\, x_{Sb} - 2793.77)$ cal mole^{-1}
$\Delta S_M^{XS} = x_{In}\, x_{Sb}\,(1.621\, x_{Sb}^3 + 2.893\, x_{Sb}^2 - 1.864\, x_{Sb} + 1.1)$ cal mole^{-1} K^{-1}

Ga–In–Sb system. The enthalpies of formation of liquid alloys have been measured for the sections $(x_{Ga}/x_{Sb}) = 3, 1, 1/2, 1/3$ with $0.08 < x_{In} < 0.7$[39]. A least-squares numerical treatment leads to the following equation for the enthalpy of formation of the liquid alloy.

$$\Delta H_M = \left(\frac{x_{Ga}}{1 - x_{In}}\,\Delta H_{Ga-In} + \frac{x_{Sb}}{1 - x_{In}}\,\Delta H_{In-Sb}\right)_{x_{In}}$$

$$+ (1 - x_{In})^2\,(\Delta H_{Ga-Sb})_{x_{Ga}/x_{Sb}} + x_{Ga}\, x_{In}\, x_{Sb}\,(\alpha\, x_{In} + \beta\, x_{Ga} + \gamma\, x_{Sb})$$

in which x_i is the ternary mole fraction of component i, ΔH_{i-j} the enthalpies of mixing, as given above, in the limiting binaries (Ga–In, In–Sb, Ga–Sb). α, β and γ coefficients equal respectively 5552.62, 5752.12 and 138.69 cal mole^{-1}.

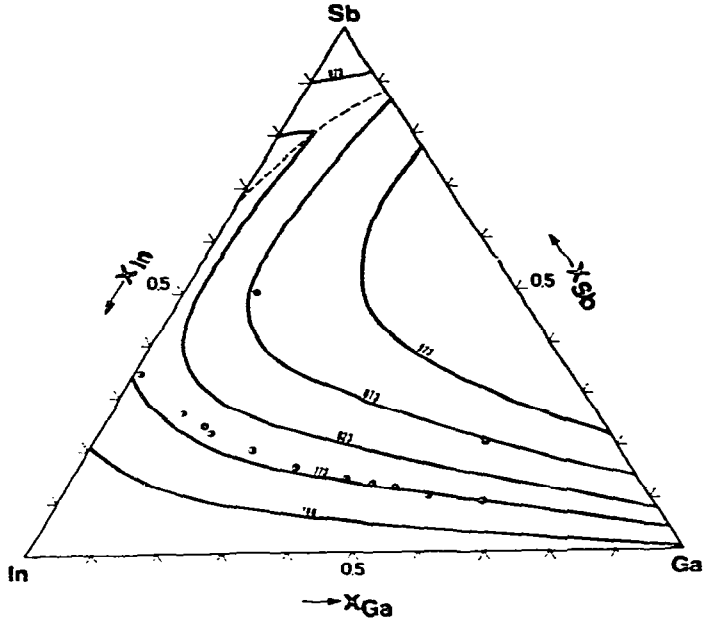

Fig. 14. Ga–In–Sb system, isothermal section at 823 K.

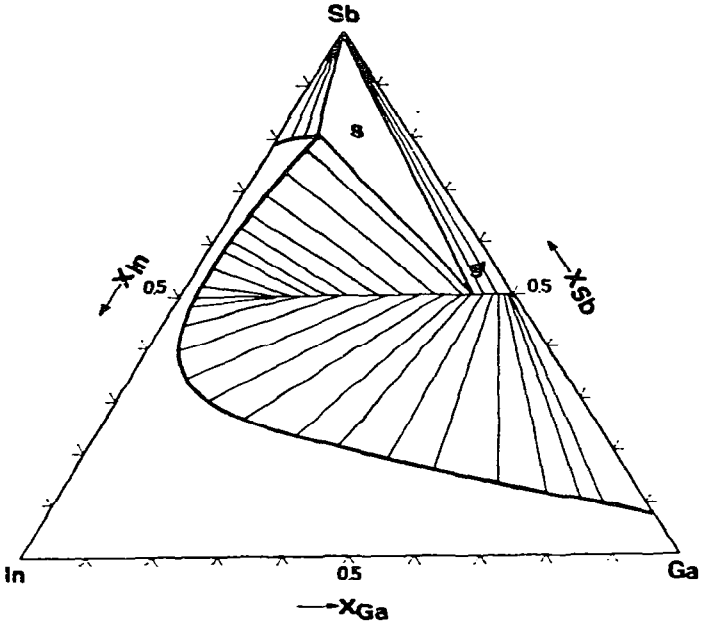

Fig. 15. Ga–In–Sb liquidus surface and experimental results.

The excess entropies of mixing ΔS_M^{XS} can be estimated by formal analogy with the previous relationship: the ΔS_{i-j}^{XS} refer to the limiting binary systems and have been given above; the α, β and γ coefficients equal zero.

Using all these data and also the equilibrium phase diagram of the GaSb–InSb quasi-binary system it was possible to calculate the Ga–In–Sb liquidus[39]. Figure 14 shows the isothermal section at 823 K of this system whereas in Fig. 15 the liquidus is plotted together with some experimental points: the agreement is very satisfactory.

CONCLUSION

Isothermal calorimetry allows us to obtain directly the enthalpy variations corresponding to the formation of simple phase liquid mixtures or liquid–liquid and solid–liquid many phase at the same time as, in some cases, the equilibrium temperatures of liquidus. We shown that these measurements are possible on a wide temperature range for two- or three-component ionic and metallic mixtures; obviously, this process can be extended to *n*-component mixtures with the usual difficulties of graphical representation.

Moreover, in the absence of a good knowledge of Gibbs enthalpies of formation and postulating some simplifying hypothesis, the liquidus lines or surfaces of the equilibrium phase diagram can often be calculated from such experimental results. If the temperatures calculated in this way agree with those obtained experimentally, it is then possible to propose a set of consistent values for the mixture under consideration.

REFERENCES

1 G. Tammann, *Z. Anorg. Chem.*, 37 (1903) 303; 45 (1905) 24; 47 (1905) 289. See also J. E. Ricci, *The Phase Rule and Heterogeneous Equilibrium*, Dover Publications, New York, 1966.
2 O. Kubaschewski and E. L. L. Evans, *La Thermochimie en Métallurgie*. Monographie Gauthier-Villard, Paris, 1964.
3 O. J. Kleppa, *J. Phys. Chem.*, 61 (1957) 1120; 64 (1960) 1542; 65 (1961) 843.
4 J. P. Bros, *Thèse doctorat d'Etat Sci. Phys.*, Marseille, 1968.
5 M. Gaune-Escard, *Thèse Doctorat d'Etat Sci. Phys.*, Marseille, 1972.
6 H. Aghai-Khafri, *Thèse Doctorat d'Etat Sci. Phys.*, Marseille, 1974.
7 H. Eslami, *Thèse Doctorat de Spécialité*, Marseille, 1976.
8 A. Tian, *C. R. Seances Soc. Biol. Paris*, 87 (1922) 869.
9 E. Calvet and H. Prat, *Microcalorimétrie*, Masson, Paris, 1955. *Récents Progrès en Microcalorimétrie*, Dunod, Paris, 1958.
10 F. E. Wittig and F. Huber, *Z. Electrochem.*, 60 (1956) 1181.
11 P. Picker, C. Jolicoeur and J. E. Desnovers, *Rev. Sci. Instrum.*, 35 (1968) 676.
12 M. Laffitte, F. Camia and M. Coten, *Bull. Soc. Chim. Fr.*, 8B (1968) 43.
13 P. Leydet, *Thèse Doctorat 3ème cycle*, Marseille, 1962.
14 B. K. Andersen and O. J. Kleppa, *Acta Chem. Scand.* Ser. A, 30 (1976) 751.
15 M. Gambino, *Thèse de Doctorat d'Etat Sci. Phys.*, Marseille, 1976.
16 R. I. Nyankovskaya, *Izvest. Akad. Nauk SSSR Ser. Fiz. Khim. Ann.*, 21 (1952) 259.
17 B. Predel, *Z. Phys. Chem. (Frankfurt am Main)*, 24 (1960) 206.
18 G. Amarell, *Dissert. Dokt. Naturwiss. Karlsruhe*, 1958.
19 F. Marco, J. Navarro and V. Torra, *J. Chem. Thermodyn.*, 7 (1975) 1059.
20 W. Koster and B. Thoma, *Z. Metallk.*, 46 (1955) 291.
21 I. G. Greenfield and R. L. Smith, *Trans. Metall. AIME*, 203 (1955) 351.
22 J. Bedmar and K. Smirous, *Czech. J. Phys.*, 5 (1955) 546.
23 M. H. Maglione and A. Potier, *J. Chim. Phys.*, 65 (1968) 1595. J. Maier and E. Wachtel, personal communication.
24 A. Yazawa, T. Kawashima and K. Itagaki, *J. Jpn. Inst. Met.*, 32 (1968) 1288.
25 B. Predel and D. W. Stein, *J. Less Common Met.*, 24 (1971) 391.
26 M. Gambino and J. P. Bros, *J. Chem. Thermodyn.*, 7 (1975) 443.
27 G. M. Blom and T. S. Plaskett, *J. Electrochem. Soc.*, 118 (1971) 1831.
28 G. A. Antypas, *J. Cryst. Growth*, 16 (1972) 181.
29 A. Joullie, R. Dedies, J. Chevrier and G. Bougnot, *Rev. Phys. Appl.*, 9 (1974) 455.

30 J. C. Wooley and B. A. Smith, *Proc. Phys. Soc. London*, 72 (1958) 214.
31 J. C. Wooley and D. G. Lees, *J. Less Common Met.*, 1 (1959) 192.
32 J. C. Wooley, B. A. Smith and D. G. Lees, *Proc. Phys. Soc. London Sect. B*, 69 (1956) 1339.
33 L. V. Nikitina and V. I. Romanenko, *Izv. Akad. Nauk SSSR*, 6 (1964) 156.
34 F. A. Trumbore, P. E. Friedland and D. A. Mills, *J. Electrochem. Soc.*, 109 (1962) 645.
35 R. Hultgren, P. D. Desai, D. T. Hawkins, M. Gleiser and K. K. Kelley, *Selected Values of the Thermodynamic Properties of Binary Alloys*, American Society for Metals, Metals Park, Novelty, Ohio, 1973.
36 J. P. Bros, *C.R. Acad. Sci.*, 263 (1966) 977.
37 J. P. Bros, R. Castanet and M. Laffitte, *C. R. Acad. Sci.*, 264 (1967) 1804.
38 F. H. Hayes and O. Kubaschewski, *J. Inst. Met.*, 97 (1969) 381.
39 I. Ansara, M. Gambino and J. P. Bros, *J. Cryst. Growth*, 32 (1976) 101.